Calame Daniel (Orcid ID: 0000-0001-6860-372X)
Herman Isabella (Orcid ID: 0000-0002-7359-6832)
Barakat Tahsin Stefan (Orcid ID: 0000-0003-1231-1562)
Tajsharghi Homa (Orcid ID: 0000-0001-8854-5213)
Alavi Shahryar (Orcid ID: 0000-0002-3484-3423)
Bahreini Seyed Amir (Orcid ID: 0000-0002-2410-6833)
Posey Jennifer E (Orcid ID: 0000-0003-4814-6765)
Marafi Dana N (Orcid ID: 0000-0003-2233-3423)
Lupski James R (Orcid ID: 0000-0001-9907-9246)

Biallelic variants in the ectonucleotidase *ENTPD1* cause a complex neurodevelopmental disorder with intellectual disability, distinct white matter abnormalities, and spastic paraplegia

Daniel G. Calame[1,2,3*], Isabella Herman[1,2,3*a], Reza Maroofian[4], Aren E. Marshall[5], Karina Carvalho Donis[6,7], Jawid M. Fatih[2], Tadahiro Mitani[2], Haowei Du[2], Christopher M. Grochowski[2], Sergio Sousa[8], Charul Gijavanekar[2], Somayeh Bakhtiari[9,10], Yoko A. Ito[5], Clarissa Rocca[4], Jill V. Hunter[3,11], V. Reid Sutton[2,3], Lisa T. Emrick[1,2,3], Kym M. Boycott[5], Alexander Lossos[12], Yakov Fellig[13], Eugenia Prus[14], Yosef Kalish[14], Vardiella Meiner[15], Manon Suerink[16], Claudia Ruivenkamp[16], Kayla Muirhead[17], Nebal W. Saadi[18], Maha S. Zaki[19], Arjan Bouman[20], Tahsin Stefan Barakat[20], David L. Skidmore[21], Matthew Osmond[4], Thiago Oliveira Silva[7, 22], David Murphy[23], Ehsan Ghayoor Karimiani[24], Yalda Jamshidi[24], Asaad Ghanim Jaddoa[25], Homa Tajsharghi[26], Sheng Chih Jin[27], Mohammad Reza Abbaszadegan[28,29], Reza Ebrahimzadeh-Vesal[29], Susan Hosseini[29], Shahryar Alavi[30], Amir Bahreini[31], Elahe Zarean[32], Mohammad Mehdi Salehi[33], Nouriya Abbas Al-Sannaa[34], Giovanni Zifarelli[35], Peter Bauer[35], Simon Robson[36], Zeynep Coban-Akdemir[2,37], Lorena Travaglini[38,39], Francesco Nicita[38,39], Shalini N. Jhangiani[40], Richard A. Gibbs[40], Jennifer E. Posey[2], Michael C. Kruer[9,10], Kristin D. Kernohan[5,41], Jonas A. Morales Saute[7,42,43], Henry Houlden[4], Adeline Vanderver[17,44], Sarah H. Elsea[2], Davut Pehlivan[1,2,3], Dana Marafi[2,45], James R. Lupski[2,3,40,46]

*These authors contributed equally.

[a]Present address:

14080 Boys Town Hospital Rd

This article has been accepted for publication and undergone full peer review but has not been through the copyediting, typesetting, pagination and proofreading process which may lead to differences between this version and the Version of Record. Please cite this article as doi: 10.1002/ana.26381

Omaha, NE 69116

Correspondence to:

James R. Lupski, MD, PhD, DSc (hon)

Department of Molecular and Human Genetics

Baylor College of Medicine

One Baylor Plaza, Room 604B

Houston, TX, 77030, USA

Tel: (713) 798-6530; Fax: +1 (713) 798-5073 Email: jlupski@bcm.edu

Clinical Correspondence: Isabella Herman (IH) isabellg@bcm.edu or Daniel Calame (DGC) calame@bcm.edu

Author affiliations

[1] Section of Pediatric Neurology and Developmental Neuroscience, Department of Pediatrics, Baylor College of Medicine, Houston, Texas, 77030, USA

[2] Department of Molecular and Human Genetics, Baylor College of Medicine, Houston, Texas, 77030, USA

[3] Texas Children's Hospital, Houston, Texas, 77030, USA

[4] Department of Neuromuscular Disorders, Queen Square Institute of Neurology, University College London, London, UK

[5] Children's Hospital of Eastern Ontario Research Institute, University of Ottawa, Ottawa, Canada

[6] Graduate Program in Genetics and Molecular Biology, Universidade Federal do Rio Grande do Sul, Porto Alegre, Brazil

[7] Medical Genetics Service, Hospital de Clínicas de Porto Alegre, Porto Alegre, Brazil

[8] Hospital Pediátrico de Coimbra, Portugal

[9] Pediatric Movement Disorders Program, Division of Pediatric Neurology, Barrow Neurological Institute, Phoenix Children's Hospital, Phoenix, AZ, 85016, USA

[10] Departments of Child Health, Neurology, and Cellular & Molecular Medicine, and Program in Genetics, University of Arizona College of Medicine–Phoenix, Phoenix, AZ, USA

[11] Division of Neuroradiology, Edward B. Singleton Department of Radiology, Texas Children's Hospital, Houston, Texas

[12] Department of Neurology, Hadassah Medical Organization and Faculty of Medicine, Hebrew University, Jerusalem 91120, Israel

[13]Department of Pathology, Hadassah Medical Organization and Faculty of Medicine, Hebrew University, Jerusalem 91120, Israel

[14]Hematology and Bone Marrow Transplantation Division, Hadassah Medical Center and the Hebrew University, POB 12000, 91120, Jerusalem, Israel

[15] Department of Genetics, Hadassah Medical Center and the Hebrew University, POB 12000, 91120, Jerusalem, Israel

[16]Department of Clinical Genetics, Leiden University Medical Centre, Leiden, The Netherlands

[17] Division of Neurology, Children's Hospital of Philadelphia, Abramson Research Center, 3615 Civic Center Boulevard, Philadelphia, Pennsylvania 19104, USA.

[18] College of Medicine / University of Baghdad, Children Welfare Teaching Hospital, Unit of Pediatric Neurology, Medical City Complex, Baghdad 10001, Iraq

[19] Clinical Genetics Department, Human Genetics and Genome Research Division, Centre of Excellence of Human Genetics, National Research Centre, El-Tahrir Street, Dokki, Cairo, Egypt, 12311

[20] Department of Clinical Genetics, Erasmus MC University Medical Center, PO Box 2040, 3000 CA, Rotterdam, The Netherlands

[21] Department of Pediatrics, Dalhousie University, Halifax, Nova Scotia, Canada.

[22] Postgraduate Program in Medicine: Medical Sciences, Universidade Federal do Rio Grande do Sul, Porto Alegre, Brazil

[23] Department of Clinical and Movement Neurosciences, UCL Queen Square Institute of Neurology, University College London, United Kingdom

[24] Genetics Section, Molecular and Clinical Sciences Institute, St. George's University of London, Cranmer Terrace, London SW17 0RE, UK

[25] Pediatric Neurology, Children Welfare Teaching Hospital, Baghdad, Iraq

[26] School of Health Sciences, Division Biomedicine, University of Skovde, Skovde, Sweden

[27] Department of Genetics, Washington University School of Medicine, St. Louis, MO, USA

[28] Medical Genetics Research Center, Medical School, Mashhad University of Medical Sciences, Mashhad, Iran

[29] Pardis Pathobiology and Genetics Laboratory, Mashhad, Iran

[30] Department of Cell and Molecular Biology & Microbiology, Faculty of Biological Science and Technology, University of Isfahan, Isfahan, Iran

[31] Department of Human Genetics, Graduate School of Public Health, University of Pittsburgh, PA, USA

[32] Department of Perinatology, Isfahan University of Medical Sciences, Isfahan, Iran

[33] Department of Pediatrics, Isfahan University of Medical Sciences, Isfahan, Iran

[34] John Hopkins Aramco Health Care, Pediatric Services, Dhahran, Saudi Arabia

[35] CENTOGENE AG, Rostock, Germany

[36] Gastroenterology and Transplantation, Departments of Medicine and Anesthesia, Beth Israel Deaconess Medical Center, Harvard Medical School, Boston, MA, USA.

[37] Human Genetics Center, Department of Epidemiology, Human Genetics, and Environmental Sciences, School of Public Health, The University of Texas Health Science Center at Houston, Houston, Texas, USA

[38] Unit of Neuromuscular and Neurodegenerative Disorders, Department of Neurosciences, Bambino Gesù Children's Hospital, IRCCS, Rome, Italy

[39]Laboratory of Molecular Medicine, Department of Neuroscience, IRCCS Bambino Gesù Children's Hospital, 00146 Rome, Italy.

[40] Human Genome Sequencing Center, Baylor College of Medicine, Houston, Texas, 77030, USA

[41] Newborn Screening Ontario, Ottawa, Canada, K1H 8L1, Canada

[42] Department of Internal Medicine, Universidade Federal do Rio Grande do Sul, Porto Alegre, Brazil

[43] Neurology Service, Hospital de Clínicas de Porto Alegre, Porto Alegre, Brazil

[44] Department of Neurology, Perelman School of Medicine, University of Pennsylvania, 3400 Civic Center Boulevard, Philadelphia, Pennsylvania 19104, USA.

[45] Department of Pediatrics, Faculty of Medicine, Kuwait University, P.O. Box 24923, 13110 Safat, Kuwait

[46] Department of Pediatrics, Baylor College of Medicine, Houston, TX, 77030, USA

Running head: *ENTPD1*-related neurodevelopmental disorder

Summary for Social Media

Twitter handle for Daniel G. Calame: @danielgcalame

Twitter handle for Isabella Herman: @isaherman85

Twitter handle for James R. Lupski lab: @LupskiLab

What is the current knowledge on the topic?

Hereditary spastic paraplegia is a progressive inherited neurological disorder caused by mutations in over 80 different genes. Because of this genetic heterogeneity, often only few affected individuals are identified for each genetic subtype, resulting in uncertainty regarding the clinical validity of gene-disease associations and the disease's phenotypic spectrum.

What question did this study address?

ENTPD1 is a gene essential in purine metabolism and has been linked to a poorly characterized hereditary spastic paraplegia (HSP), SPG64, with only a few affected individuals identified throughout the world. We set out to examine a large cohort of patients with ENTPD1-related neurological disorder to fully evaluate the disease spectrum and molecular mechanisms underlying disease pathogenicity.

What does this study add to our knowledge?

Through the identification of 17 previously unreported families with 27 affected individuals and 12 novel *ENTPD1* variants, this study firmly establishes the gene-disease validity of *ENTPD1* as the cause of an autosomal recessive (AR) complex HSP characterized by childhood onset, developmental delay/intellectual disability (DD/ID), dysarthria, progressive spastic paraplegia, dysmorphic features, cerebral white matter abnormalities, and developmental regression. We additionally identify multiple clinical diagnostic biomarkers including 1) T2-hyperintense signal in the posterior limb of the internal capsule (PLIC) on brain MRI, 2) diminished ENTPD1/CD39 staining on peripheral blood cells by flow

cytometry and peripheral nerve biopsies by immunohistochemistry, 3) diminished ATP and ADP breakdown in a lymphoblast-based cellular assay, and 4) show that ENTPD1 deficiency leads to alteration in lipid, nucleotide, and energy metabolism.

How might this potentially impact the practice of Neurology?

Defining the full genotypic and phenotypic spectrum of rare neurological disease traits like SPG64 is essential for clinical management and patient and family counseling. Expansion of the allelic spectrum and development of new diagnostic biomarkers will facilitate earlier recognition of SPG64, act as a springboard for additional mechanistic studies of the role of purine metabolism in neurodevelopment and neurodegeneration, and aid therapeutic investigations.

Abstract

Objective: Human genomics established that pathogenic variation in diverse genes can underlie a single disorder. For example, hereditary spastic paraplegia (HSP) is associated with over 80 genes with frequently only few affected individuals described for each gene. Herein, we characterize a large cohort of individuals with biallelic variation in *ENTPD1*, a gene previously linked to spastic paraplegia 64 (MIM# 615683).

Methods: Individuals with biallelic *ENTPD1* variants were recruited worldwide. Deep phenotyping and molecular characterizations were performed.

Results: A total of 27 individuals from 17 unrelated families were studied; additional phenotypic information was collected from published cases. Twelve novel pathogenic *ENTPD1* variants are described: c.398_399delinsAA; p.(Gly133Glu), c.540del; p.(Thr181Leufs*18), c.640del; p.(Gly216Glufs*75), c.185T>G; p.(Leu62*), c.1531T>C; p.(*511Glnext*100), c.967C>T; p.(Gln323*), c.414-2_414-1del, and c.146 A>G; p.(Tyr49Cys) including four recurrent variants c.1109T>A; p.(Leu370*), c.574-6_574-3del, c.770_771del; p.(Gly257Glufs*18), and c.1041del; p.(Ile348Phefs*19). Shared disease traits include: childhood-onset, progressive spastic paraplegia, intellectual disability (ID), dysarthria, and white matter abnormalities. *In vitro* assays demonstrate that *ENTPD1* expression and function are impaired and that c.574-6_574-3del causes exon skipping. Global metabolomics demonstrates ENTPD1 deficiency leads to impaired nucleotide, lipid, and energy metabolism.

Interpretation: The *ENTPD1* locus trait consists of childhood disease-onset, ID, progressive spastic paraparesis, dysarthria, dysmorphisms, and white matter abnormalities with some individuals showing neurocognitive regression. Investigation of an allelic series of *ENTPD1*: i) expands previously described features of *ENTPD1*-related neurological disease, ii) highlights the importance of genotype-driven deep phenotyping, iii) documents the need for global

collaborative efforts to characterize rare AR disease traits, and iv) provides insights into the disease trait neurobiology.

Introduction

Genome sequencing and clinical genomics have markedly improved molecular diagnostic rates in rare Mendelian disorders by accelerating novel disease gene and variant allele discovery and expanding the phenotypic spectrum associated with known disease genes[1-3]. This progress resulted in the understanding that single families of disorders can be caused by pathogenic variation in genes with diverse functions. For example, hereditary spastic paraplegias (HSP) are a group of neurological disorders affecting 1.8 in 100,000 individuals globally[4]. Inheritance patterns for HSP disease traits are variable, including autosomal dominant (AD), autosomal recessive (AR), X-linked, *de novo*, and mitochondrial inheritance[5]. Despite shared features, HSP results from pathogenic variation in over 80 genes/loci involved in mitochondrial functioning, lipid metabolism, vesicle/axonal trafficking, and myelination. With the rapid pace of disease gene discovery, this number is anticipated to expand. In fact, an "HSPome" of known HSP disease genes, candidate disease genes, and proximal interactors has implicated almost 600 potential HSP genes[6].

HSP is classified into "pure" and "complex/complicated" with unifying features of corticospinal tract nerve axonopathy, progressive gait difficulty, and axonal length-dependent neuropathy[7,8]. Complex HSP additionally encompasses developmental delay/intellectual disability (DD/ID), structural brain abnormalities, ataxia, epilepsy, amyotrophy, and visual abnormalities[8]. Consequently, complex HSP frequently overlaps with neurodevelopmental disorders (NDD); e.g. leukodystrophies, cerebellar ataxias, and syndromic DD/ID[9].

As with hereditary neuropathies[10], the allelic spectrum of HSP is unevenly distributed across known disease genes. For example, pathogenic variation in *SPAST*, the cause of AD spastic paraplegia 4 (MIM# 182601), accounts for approximately 60% of HSP diagnoses[11-14]. The abundance of AD spastic paraplegia 4 and other "common" HSP causes reflects historical population-specific events, e.g. founder effect, population bottlenecks, or high frequency

mutational events occurring as a consequence of genomic architecture, e.g. *Alu/Alu*-mediated rearrangements (AAMRs) due to abundance of *Alu* repetitive elements and genomic instability within *SPAST*[15].

The remaining allelic spectrum of HSP exhibits extensive molecular heterogeneity and is a collection of ultra-rare diseases, often with only a few individuals described for each gene locus. Studies investigating the phenotypic spectrum from different families and ethnicities worldwide and diverse pathogenic variant alleles, i.e., an allelic series, are often lacking. For example, AR spastic paraplegia type 64 (SPG64, MIM #615683) due to biallelic pathogenic variation in *ENTPD1*, the gene encoding the ectonucleosidase ENTPD1 involved in adenosine triphosphate (ATP) hydrolysis, has been described in only a few individuals with limited and seemingly dissimilar phenotypic characterization[6,16-18]. Affected individuals have shared features of childhood-onset disease with progressive spastic paraplegia, DD/ID, and variable findings of brain abnormalities and abnormal reflexes ranging from areflexia to hypo-and hyperreflexia. It is therefore critical to deeply phenotype large cohorts of individuals with rare diseases, e.g. due to biallelic *ENTPD1* variants, potentially revealing previously undescribed features (e.g. phenotypic expansion and multilocus pathogenic variation, MPV), and therefore providing a comprehensive understanding of the disease process and gene-associated trait.

Herein, we describe phenotypic and molecular features of a large cohort of individuals with biallelic variants in *ENTPD1* and provide evidence for a complex neurodevelopmental disorder (NDD) with progressive spastic paraplegia with previously unrecognized clinical features.

Materials and methods

Patient identification and recruitment

This study was approved by the Institutional Review Board (IRB) at Baylor College of Medicine (Protocol H-29697) or through other collaborative local IRBs. Additional affected participants were identified through GeneMatcher[19] or personal communication. Written consent, including consent for publication of photographs, was obtained for all participants. Study participants were examined by a clinical geneticist and/or neurologist and phenotypic features were described using Human Phenotype Ontology (HPO) terms[20]. Brain magnetic resonance images (MRIs) were retrospectively reviewed and analyzed by a single observer; board certified neuroradiologist (JVH).

Exome sequencing

For family 1, trio exome sequencing (ES) was performed at the Human Genome Sequencing Center (HGSC) at Baylor College of Medicine (BCM) through the Baylor-Hopkins Center for Mendelian Genomics (BHCMG) initiative as previously described[21]. For all other identified families, ES was performed by local institutions or commercial clinical molecular diagnostic laboratories via previously established protocols[22].

Absence of heterozygosity

BafCalculator (https://github.com/BCM-Lupskilab/BafCalculator)[2], an in-house developed bioinformatic tool that extracts the calculated B-allele frequency (ratio of variant reads/total reads) from unphased exome data, was used to calculate genomic intervals and total genomic content of absence of heterozygosity (AOH) intervals as a surrogate measure for runs of homozygosity (ROH) likely representing identity-by-descent (IBD) genomic intervals. B-allele frequency was transformed by subtracting 0.5 and taking the absolute value for each data point before being processed by circular binary segmentation using the DNAcopy R Bioconductor package.

Confirmation of alternative splicing

Whole blood RNA from family 5 was extracted using the PAXgene Blood RNA kit (Qiagen, Germantown, MD) according to the manufacturer's instructions and cDNA was synthesized using the High-Capacity cDNA Reverse Transcription kit (Applied Biosystems, Foster City, CA) with poly-dT (20) primers according to manufacturer's protocol. Amplicons were generated from control, proband, and parental cDNA using HotStartTaq DNA polymerase (Qiagen, Germantown, MD) according to manufacturer's protocol. DNA bands at various sizes were excised, purified via the PureLink PCR purification and gel extraction kit (Invitrogen, Carlsbad CA), and Sanger dideoxy DNA sequencing implemented at the BCM sequencing core facility.

Real-time PCR

Immortalized lymphoblast cell lines from affected individuals were established from blood samples at The Centre for Applied Genomics (Toronto, Canada). Total RNA was obtained from affected and control lymphoblast cell lines with the RNeasyMinikit (Qiagen, Germantown, MD) and reverse transcribed into complementary DNA (cDNA) with iScript kit (BioRad Laboratories, Hercules, CA) according to manufacturer's protocol. cDNA was amplified with gene-specific primers and iQ SYBR Green Supermix (BioRad Laboratories, Hercules, CA) and read on a CFX96 Touch Real-time PCR Detection System. Gene expression was quantified using the standard Ct method with CFX software, and all data corrected against *GAPDH* as an internal control.

Western blot analysis

Cells were lysed in radioimmunoprecipitation assay buffer containing aprotinin, phenylmethanesulfonyl fluoride, and leupeptin at a final concentration of 10 mg/ml each in the composite solution (Sigma-Aldrich, St. Louis, MO) and concentrations were determined by Bradford assay (BioRad Laboratories, Hercules, CA). Protein samples were resolved by

standard SDS-PAGE, transferred onto nitrocellulose membrane, incubated in blocking, followed by overnight incubation with primary antibody (ENTPD1, Abcam ab108248). Membranes were washed and incubated with secondary antibody (HRP conjugated anti-rabbit; BioRad Laboratories). Blots were visualized by chemiluminescence using the Clarity Western ECL substrate (BioRad Laboratories). Control protein was extracted from healthy, unrelated, age-matched control cell lines.

ATPase and ADPase assay

A total of 250,000 lymphoblasts were harvested per technical replicate from each cell line. The cells were washed and each replicate plated in a single well of a round bottom 96-well plate. Cells were then incubated with either 10 mM ADP or 10 mM ATP, or left untreated, for 30 min at 37°C. The supernatant was transferred to a new, flat bottom 96-well plate and phosphate concentration was measured using the Malachite Green Phosphate Assay kit (Sigma-Aldrich, St. Louis, MO) according to the manufacturer's instructions. The normalized phosphate production reported is fold change relative to untreated samples.

Flow Cytometry

Blood samples were collected in 3 ml EDTA tubes and analyzed for immune cell subsets using the following surface markers: CD16, CD56, CD3, CD4, CD8, CD2, CD15, CD19, CD20, HLA-DR, CD39 and CD73. All samples were analyzed using Beckman Coulter dual Laser Navios Flow Cytometer equipped with 488nm Argon and a 635 nm-diode laser, allowing six color fluorescence data acquisition (Beckman Coulter, Inc., 250 S., Kraemer Blvd, Brea, CA).

Sural nerve biopsy

Paraffin embedded sural nerve biopsy sections of the patient and a control sample were stained immunohistochemically for CD39 (Leica/Novocastra, 1cc, clone NCL-CD39, LOT-6017994, 1:50), according to the manufacturer's instructions and standard staining protocols.

Untargeted metabolomic analyses

Clinical untargeted metabolomics was performed under an IRB-approved research protocol (H-35388) by Baylor Genetics and Metabolon, Inc., as previously described[23-27]. EDTA plasma samples were collected from Family 6 (P8, P9) and Family 9 (P15), frozen, and shipped on dry ice overnight and kept at -80C until analyzed, as previously described [23,25-27]. Molecules were identified and z-scores generated relative to the reference population. An average of 798 +/- 7 metabolites were detected in the plasma of each of the 3 patient samples analyzed. Due to the age range of the subjects in this study, androgenic, pregnenolone, and progestin steroids were excluded from the analysis. Also excluded were known prescription medications, over the counter drugs and/or supplements, and partially-characterized molecules, leaving ~773 molecules for further assessment. These metabolomics datasets for each patient were collated, and samples were filtered to identify metabolites that were altered in patient biofluids with z-score > +1.5 or < -1.5 and in the top 10% or bottom 10% of all cases in the laboratory clinical testing database. Molecules absent in the patient sample but detected in the batch analysis and typically detected in >90% of patient samples were reviewed for possible contribution to the biochemical phenotype. Specific molecules altered in at least 2 out of the 3 patient samples were further analyzed to highlight key metabolic features. Metabolite enrichment and network analyses were performed by using MetaboAnalyst 5.0 (https://www.metaboanalyst.ca) using the integrated gene-metabolic pathways network analysis with the metabolite–KEGG interaction network.

Results

Index proband

The index patient (P1, family 1; **Fig. 1A**) is an eight-year-old girl referred to the Baylor-Hopkins Center for Mendelian Genomics (BHCMG) for DD/ID, spastic paraplegia and progressive gait impairment. Concerns about the proband's development arose due to delayed walking after 2 years of age. At three years, she developed spastic paraplegia. Her neurological examination at 8 years showed dysarthria, muscle weakness with amyotrophy, and hyperreflexia in the upper extremities with areflexia in the lower extremities (**Table S1**). Trio ES revealed a novel homozygous variant in *ENTPD1*, NM_001776.6: c.398_399delinsAA; p.(Gly133Glu) (**Fig. 1A**). The variant is absent from gnomAD, is only found in this family in our research database of >13,000 exomes, and the affected amino acid residue is fully conserved across species. *ENTPD1*: c.398_399delinsAA is located in an 11.1 Mb AOH block and the total AOH size of the proband is 310 Mb, consistent with the offspring of a first cousin mating (**Fig. 1B**).

Recruitment of additional families with biallelic *ENTPD1* variation

Given limited phenotypic characterization of *ENTPD1*-related neurological disease, we identified a total of 17 unrelated families with 27 affected individuals through GeneMatcher (https://genematcher.org/)[21] and communication with neurogenetic research laboratories from around the globe (**Fig. 1C, Table S1**). Families were from diverse countries, including Turkey (Family 2), Brazil (Families 3, 4, and 5), Puerto Rico (Family 6), Poland (Family 7), Israel (Family 8), Portugal (Family 9), Persia (Families 10, 11, 12, 15, 16, 17), Egypt (family 13), and the Dominican Republic (Family 14). Review of the literature revealed an additional five families with nine affected individuals (**Table S1**)[6,16-18].

Phenotypic spectrum of *ENTPD1*-related neurological disease

Comparison of phenotypic features using HPO terminology[22] among all affected individuals revealed both major similarities as well as differences, suggestive of a phenotypic spectrum with a 'clinical synopsis' of shared commonalities (**Table 1, Table S1**). The average age of the cohort at last examination was 16 years (range 3-32 years, median 15 years). All affected individuals had symptom onset in early childhood, DD/ID, and progressive spastic paraplegia with impaired ambulation. Behavioral abnormalities, including attention-deficit hyperactivity disorder (ADHD), aggression, and stereotypies were common, as was neurocognitive and language regression. DD/ID was diagnosed in clinical or education settings due to deficits in intellectual and adaptive functioning. Neurocognitive regression was determined by a progressive decline in functioning not attributable to progressive spastic paraplegia.

The neurological examination revealed dysarthria (27/36), axial hypotonia (7/36), amyotrophy (9/36), and weakness (28/36). Abnormal reflexes were common and included hyperreflexia (8/36), hyporeflexia (5/36), and areflexia (3/36). A total of 20 individuals had both hyperreflexia and hypo/areflexia, consistent with mixed upper and lower motor neuron dysfunction. Additionally, a total of 12 individuals had electromyography/nerve conduction studies (EMG/NCS). Two cases with areflexia showed findings consistent with motor axonal neuropathy (P12 and 13), one case with hyporeflexia showed myopathic findings (P16), and two cases with hyporeflexia showed findings consistent with polyradiculopathy and motor axonal neuropathy, respectively (P21 and 32). In the seven cases with normal electrodiagnostic studies, two were hyperreflexic, three cases showed a mixed picture of upper and lower motor neuron signs, and two individuals did not have reflexes documented (**Table S1**). For individuals who did not have EMG/NCS performed, neuropathy was determined by clinical signs and symptoms including absent or decreased reflexes, impaired sensation, and neuropathic pain. Dysmorphic facies were common (13/36) and included low anterior hairline,

synophrys, low-set ears with fleshy lobes, prominent philtrum, and mild micrognathia (**Fig. 2A**). Centripetal obesity, scoliosis, and genu valgus were observed (**Fig. 2B**). Additional musculoskeletal abnormalities included camptodactyly, spatulated and tapered fingers, broad toes, and *pes cavus* and *planus,* and scoliosis (**Fig. 2C-I**). Hip x-rays were generally unremarkable with normal bone structure (**Fig. 2J**).

ENTPD1-related neurological disease causes MRI abnormalities

As previous reports of affected individuals with biallelic pathogenic *ENTPD1* variants described brain white matter abnormalities in only two of nine affected individuals[6], we sought to better characterize neuroimaging features of the *ENTPD1*-related disease trait. Brain MRI images were available for ten individuals and were reviewed by a board certified pediatric neuroradiologist (**Fig. 3A-G**). For 18 individuals an MRI report was provided, and eight individuals did not have any neuroimaging. Abnormalities of the MRI included white matter and corpus callosum findings, cerebellar atrophy, and abnormal signal in the posterior limb of the internal capsule

Thinning of the corpus callosum was present in three individuals (P4, 9, 21) and predominantly affected the isthmus (**Fig. 4B-E**). White matter abnormalities were observed in 15/28 patients for whom a brain MRI was performed. Of these, 12 individuals had persistent T2 signal abnormalities in the posterior limb of the internal capsule (PLIC). Review of a previously published individual (P34)[17] not initially reported to have brain MRI abnormalities was subsequently found to have abnormal T2 signal hyperintensity in the PLIC at 15 years of age (**Fig. 3G**). Cerebellar atrophy was observed in 3 individuals (P19, 20, 23).

Biallelic pathogenic *ENTPD1* variants identified in this cohort

ENTPD1 is located on chromosome 10 and contains 10 exons; the major annotated canonical transcript is NM_001776.6 (ENST00000371205.5). Previous reports identified five distinct *ENTPD1* variants with two missense and three predicted loss-of function (LoF) variant alleles: c.628G>A; p.(Gly210Arg), c.520G>T; p.(Glu174*), c.401T>G; p.(Met134Arg), c.970C>T; p.(Gln324*), and c.978del; p.(Gly327Lysfs*40)[6,16-18]. We describe 12 novel variants (**Fig. 4A, B**) of which 10 are LoF: c.540del; p.(Thr181Leufs*18), c.640del; p.(Gly216Glufs*75), c.1109T>A; p.(Leu370*), c.185T>G; p.(Leu62*), c.1531T>C; p.(*511Glnext*100), c.967C>T; p.(Gln323*), c.770_771del; p.(Gly257Glufs*18), c.1041del p.(Ile348Phefs*19), c.414-2_414-1del, and c.574-6_574-3del. c.1531T>C; p.(*511Glnext*100) is a stoploss variant, predicted to result in a 100 amino acid extension on the 522 amino acid ENTPD1 protein. The ENTPD1 protein has two catalytically active transmembrane domains on the N and C terminus[28] and this large extension is likely to disrupt the C terminus transmembrane domain, resulting in impaired catalytic activty. Additionally, one missense variant c.146 C>G; (p.Tyr49Cys) and one multinucleotide variant resulting in a single amino acid substitution, c.398_399delinsAA; p.(Gly133Glu) were identified (**Fig. 4A, B**).

All variants are ultra-rare[29] and absent from gnomAD. The exception, c.1109T>A; p.(Leu370*), is found in two heterozygotes of European non-Finnish descent; but it is important to note the bias of European descent genomes in the gnomAD database. All variants are predicted damaging by *in silico* analysis (**Table 1**).

Intronic splicing variant results in alternative splicing and exon skipping

The majority of *ENTPD1* variant alleles identified in this study are LoF variants predicted to undergo nonsense mediated decay (NMD) or result in a truncated protein (**Fig.**

4B)[30]. However, the impact on gene function of the intronic variant c.574-6_574-3del was unclear. As the variant falls within intron 5, we hypothesized it causes aberrant splicing via either exon skipping, intron inclusion or a combination of both. To test this hypothesis, cDNA was synthesized from control, homozygous proband (P15), and heterozygous carrier parents and amplified using separate primer pairs for exons 4-7 and exons 6-10 (**Fig. 5A**). Amplification of exons 4-7 showed an 818 bp product in wildtype control and heterozygous parent but not the homozygous affected proband (**Fig. 5B**). Sanger dideoxynucleotide DNA sequencing confirmed that this product contains exons 4, 5, 6, and 7. Furthermore, the proband showed a 572 bp product absent from the control and parental samples. Sanger sequencing of the 572 bp product showed exons 4, 5, 7 and complete absence of exon 6, evidence confirming exon skipping in the affected proband. As a second confirmatory step of exon 6 skipping in the proband, primers for exon 6 and exon 10 were used for amplification (**Fig. 5C**). In the control and parental samples, an 861 bp PCR product was detected with Sanger sequencing confirming presence of exons 6, 7, 8, 9, and 10. No amplification was present in the proband P7, consistent with absence of cDNA transcript including exon 6.

Biallelic *ENTPD1* variants impair ATP hydrolysis and ENTPD1 expression

Given that ENTPD1 is an essential enzyme in the hydrolysis of ATP to ADP and ADP to AMP (**Fig. 6A**), we next tested the effect of the homozygous *ENTPD1* missense variant c. 401T>G; p.(Met134Arg) on ATP/ADP metabolism. Patient lymphoblasts were obtained from family 20 (P32 and P33) (**Fig. 6B**). Quantitative PCR of control and proband samples revealed significantly decreased mRNA levels in both affected individuals compared to control with approximately 50% reduction (**Fig. 6C**). Western blot analysis of ENTPD1 protein showed a substantial reduction in the predominant, higher molecular weight/relative molecular mass (M_r)

band compared to control individuals with concurrent increase in the intensity of the lower weight band. However, overall ENTPD1 protein levels were still markedly decreased in the affected individuals compared to controls (**Fig. 6D**).

To test the functional effect of altered ENTPD1 protein expression on ATP and ADP hydrolysis, ATPase and ADPase activity of proband samples were measured using normalized phosphate production as a readout. This experiment showed significantly decreased phosphate production in lymphoblasts obtained from P32 and P33, consistent with impaired ATP/ADP hydrolysis (**Fig. 6E**). Given that ENTPD1 is highly expressed in lymphocytes and polymorphonuclear leukocytes (PMNs), flow cytometry was performed on whole blood from P12, P13, which showed complete absence of ENTPD1+ cells (**Fig. 6F**). Furthermore, immunohistochemistry for ENTPD1 on paraffin sections of sural nerve from P12 showed complete absence of endo- and epineural vascular staining, indicating lack of ENTPD1 expression (**Fig. 6G**).

Untargeted metabolomics identifies perturbations in nucleotide, lipid, and energy metabolism

Purinergic signaling is an important regulator of cellular metabolism and inflammation. Ectonucleotidase deficiency in mouse models causes hepatocellular dysfunction, impaired glucose homeostasis, intestinal inflammation, and microbiome alterations [31]. Therefore, we explored the impact of ENTPD1 deficiency on metabolic homeostasis using untargeted metabolomics. Integrated gene-metabolic pathways network analysis (**Fig. 7**) revealed consistent patterns of metabolic abnormalities in plasma samples from three subjects. Metabolic alterations revealed multiple alterations in nucleotide, carbohydrate, and lipid metabolism with 37 molecules altered in at least two of three patient samples. When

considering broader biochemical pathways, ~140 molecules were perturbed within the same metabolic networks (**Fig. 7**). These data point to significant roles for ENTPD1 and purinergic signaling in metabolic homeostasis. In each sample, multiple endocannabinoids and related metabolites were altered, perhaps indicating an elevated inflammatory state[32]. Many alterations involved metabolites associated with liver dysfunction, such as bilirubin, multiple altered long chain fatty acids and glycerophospholipids. Furthermore, several reported biomarkers associated with obesity, insulin resistance, and metabolic syndrome were identified in all patient samples, including elevations of 3-ketosphinganine, glucose, and N-acetylated amino acids, as well as low fructose.

Discussion

ENTPD1 was first identified as a candidate disease gene for AR DD/ID[33] and subsequently linked to SPG64 (MIM# 615683)[6,16-18]. These individuals had overlapping features of spastic paraplegia and DD/ID, but were highly variable in other neurological symptoms (**Table S1**). Deep phenotyping of all identified *ENTPD1* patients herein delineated a clinical synopsis of: childhood disease onset, DD/ID, spastic paraplegia, dysarthria, neurocognitive regression, dysmorphic facies, and white matter abnormalities (**Table 1, Table S1**). Given the progressive nature and potential neurodegenerative process accompanying *ENTPD1*-related disease, natural history studies and longitudinal follow up will be required to better understand this disease trait.

Mixed upper and lower motor neuron findings in *ENTPD1*-related neurologic disorder

Several cases of SPG64 had clinical features and electrodiagnostic findings suggestive of combined upper and lower motor neuron dysfunction[6,18]. Here, we expand upon these preliminary observations, demonstrating additional cases with findings consistent with both

upper and lower motor neuron dysfunction and neuropathy. Of the twenty-five cases for which details of reflex examination are available, 40% show a mixed picture, 36% hyporeflexia/areflexia, and 24% hyperreflexia. Areflexia/hyporeflexia is not typical of 'classic' HSP as upper motor neuron degeneration results in loss of inhibitory descending pathways with resultant exaggeration of the stretch reflex. However, several HSP subtypes exhibit features of mixed upper and lower motor neuron dysfunction (e.g. SPG3, 7, 30, 31), and some have neuropathy as a major clinical feature (e.g. SPG 15, 20, 26, 35, 39).

While EMG/NCS was only performed in a subset of cases, 30% had evidence of motor axonal neuropathy, confirming involvement of the peripheral nervous system in SPG64. One potential explanation is ATP/ADP accumulation due to impaired hydrolysis triggers excitotoxicity within the central and peripheral nervous system with greater impact on the CNS, resulting in an upper motor neuron syndrome with variable lower motor neuron dysfunction. The observation of myopathic findings in a single case is also curious and may reflect an impact of ENTPD1 deficiency on both the nervous system and skeletal muscle. Alternatively, since the individual in question originates from a consanguineous family, she may have a dual molecular diagnosis resulting from multilocus pathogenic variation and a blended myopathy-HSP phenotype, a finding seen in ~20-30% of consanguineous families[3].

White matter abnormalities in *ENTPD1*-related neurological disease

A remarkable feature of *ENTPD1*-related neurological disease is the unique pattern of white matter abnormalities and persistent T2 signal hyperintensities in the PLIC. Persistent signal abnormalities in the PLIC have previously been reported in a specific disorder of purine metabolism due to biallelic variants in *ITPA* [34]. This is especially intriguing given that *ENTPD1* is intricately involved in purine metabolism as an ectonucleotidase and the neuroimaging

findings observed in many of our patients are strikingly like those seen with *ITPA*. It is therefore possible that PLIC signal abnormality constitutes a pathognomonic finding of diseases affecting purine metabolism.

Spectrum of pathogenic biallelic *ENTPD1* variants

We identified 12 previously unpublished variants, the majority of which are predicted likely damaging and to cause LoF. Additionally, one missense variant c.146 C>G; (p.Tyr49Cys) and one multinucleotide variant causing a single amino acid substitution were uncovered. Double missense variants, a type of multi-nucleotide variant (MNV), are rare but occur due to replication error introduced by DNA polymerase zeta (pol-zeta) during DNA damage repair and translesion DNA synthesis[35]. Four recurrent variants were identified including c.574-6_574-3del found in families 5 (Brazilian, homozygous), 6 (Puerto Rican, compound heterozygous), and 9 (Portuguese, homozygous); c.770_771del in families 3 and 4 (both Brazilian, homozygous); c.1041del in families 15 and 16 (both Persian, homozygous); c.1109T>A in families 7 (Poland, homozygous) and families 10, 12, 17 (Persian, homozygous). The observation that c.574-6_574-3del and c.770_771del were found in the homozygous state in unrelated consanguineous families from countries with substantial Portuguese ancestry (Brazil and Portugal) may suggest these variants represent founder alleles from the Iberian peninsula homozygosed through clan genomics IBD or population/geographic isolation[36,37]. Alternatively, the *de novo* variant allele may be a recurrently derived new mutation in antecedent generations of each clan. Similarly, the LoF variant c.1041del was found in families 16 and 17 may represent a founder allele in Persia, whereas the stop gain variant c.1109T>A; p.(Leu370*) found in four unrelated families from Persia and Poland, consistent with a recurrent mutation.

Aberrant splicing in neurological disease

Given that the splicing variant c.574-6_574-3del was identified in multiple unrelated families, we hypothesized pathogenicity based on aberrant splicing and found that exon 6 skipping indeed occurs in a proband harboring this variant in the homozygous state (**Fig. 5**). *ENTPD1* has 13 recognized splice variants of which four are protein coding[38]. The aberrant splice product observed in our studies has not been reported to occur in normal tissue[38]. Identification of the splicing defect caused by the recurrent variant c.574-6_574-3del provides an opportunity for nucleic acid based-molecular therapeutic intervention using antisense oligonucleotides (ASOs) and/or small interfering RNA (siRNA) molecules[39].

Function of ENTPD1 in health and disease

ENTPD1, ectonucleoside triphosphate diphosphohydrolase 1 (MIM*601752) is the prototype ecto-nucleoside triphosphate diphosphohydrolase of the CD39 family involved in extracellular ATP and ADP phosphohydrolysis. Given the modulatory roles in purine metabolism and purinergic signaling, ENTPD1 expression by glial cells is important in the central nervous system, where it plays an essential role in regulating neuronal activity[40]. ATP is stored in neuronal synaptic vesicles and glial cells together with classic neurotransmitters, e.g. GABA and glutamate, and is released by exocytosis upon neuronal stimulation[41]. High concentrations of ATP trigger neurotoxicity through the purinergic receptor P2X7 and are implicated as potential therapeutic targets in motor neuron diseases and Charcot-Marie-Tooth disease type 1A[42,43].

ENTPD1 plays an important role in the cell-surface catabolism of ATP (**Fig. 6A**). A previous study using nuclear magnetic resonance spectroscopy (NMR) reported that the LoF

variant c.185T>G; p.(Leu62*) found in family 8 in this report affects ENTPD1 enzymatic function with impaired ATP and ADP hydrolysis [44]. Here, we provide evidence from flow cytometry and immunohistochemistry, two clinically accessible tests, that the previously reported impairment of ATP/ADP metabolism caused by the *ENTPD1* variant c.185T>G is likely a consequence of the complete absence of ENTPD1 protein *in vivo* (**Fig. 6E, F**).

ENTPD1 is a highly glycosylated protein and alterations in glycosylation affect electrophoretic mobility, stability, and enzymatic activity[45]. Therefore, it is likely the overall reduction in ENTPD1 protein levels as well as the relative increase in the lower molecular weight species may reduce ENTPD1 stability and/or impair ATP/ADPase activity, disturbing purinergic neurotransmission and/or causing neurotoxicity as potential disease mechanism. Similarly, the LoF variant c.185T>C; p.(Leu62*) resulted in absence of ENTPD1 in the vasculature of the epi/perineurium with possible implications for peripheral nerve health and function (**Fig. 6G**).

Furthermore, an *in vitro* studies using a cellular model of sympathetic neurons demonstrated that ENTPD1 modulates exocytotic and ischemic neurotransmitter release[46] and targeted LoF *Entpd1*$^{-/-}$ mouse models exhibit a pro-epileptogenic phenotype[47]. Given the important cellular function of ENTPD1 and its ubiquitous expression, it is possible that impaired ENTPD1 function could have extra-CNS manifestations. For example, LoF *Entpd1* mouse models exhibit impaired hemostasis and thromboregulation due to platelet dysfunction and hepatic insulin resistance[48-50]. While platelet dysfunction or glucose intolerance was not identified in our cohort, untargeted plasma metabolomic analysis in three affected individuals demonstrated consistent patterns of metabolite abnormalities indicating dysfunctional nucleotide, lipid, and energy metabolism. Several alterations were suggestive of subclinical liver dysfunction, an elevated inflammatory state, and abnormal glucose metabolism and may warrant clinical surveillance. Finally, these abnormalities may represent a 'metabolomic

signature' of ENTPD1 deficiency, which could prove a useful diagnostic or therapeutic biomarker. The full extent of these perturbations across the lifespan and clinical significance remains to be determined.

Treatment and development of therapeutics

The HSPs constitute a spectrum of progressive neurological disorders with only supportive therapies to ameliorate or mitigate disease[5]. A major challenge in therapeutic development stems from the diverse molecular pathways with over 80 HSP disease genes notifiedied to date. Another challenge in the evaluation of potential therapeutics is the insidious and progressive nature of the disease, leading to challenges in therapeutic endpoints and efficacy assessments. Nevertheless, with current advances in genome medicine and evolving understanding of molecular disease etiology, therapeutic development targeting diverse molecular disease mechanisms are now feasible. Accurate and timely molecular diagnosis and natural history studies will greatly facilitate clinical trials. The known role of ENTPD1 in ATP breakdown and our experimental evidence of impaired ATP/ADP hydrolysis in patients with *ENTPD1*-related neurological disease suggests antagonism of the purinergic receptor P2X7 may be a worthwhile target for therapeutic intervention.

Limitations of this study include its reliance on retrospective chart review and diverse clinical evaluations precluding use of HSP specific metrics such as the Spastic Paraplegia Rating Scale (SPRS) which could help gauge longitudinal disease severity and progression[51]. Formal neuropsychiatric testing was either not performed or results were unavailable, limiting more precise characterization of the degree of intellectual disability. Similarly, only a subset of the cohort underwent electrodiagnostic evaluation or had MRIs available for retrospective review. Finally, replication of our ADPase/ATPase assay, ENTPD1 immunostaining, and

global metabolomics analysis in additional patients would help strengthen validity of these tests as diagnostic biomarkers.

In conclusion, we establish *ENTPD1* as the etiology of a complex neurodevelopmental disorder in the HSP spectrum characterized by intellectual disability, white matter abnormalities, and progressive spastic paraplegia. Allelic series and detailed phenotyping in rare neurological disease can capture a more comprehensive spectrum of disease and define disease traits. Moreover, such information provides recurrence risk and prognostic information for family counseling, establishes pathophysiological mechanisms, provides neurobiological insights, and may ultimately lead to the development of novel therapeutic options for rare neurological disorders based on shared molecular features. Future endeavors should involve the development of diagnostic biomarkers with the goals of early disease screening, as a readout of disease activity, and as a measure of treatment response for SPG64.

Acknowledgements

We thank the families reported in this study for their willingness to contribute to the advancement of science and the understanding of rare neurological disease. Ms. Liat Ben Avi is thanked for her technical assistance.

The initial stages of this project and preliminary data were previously presented in poster form at the American Society of Neurology Annual Meeting in April 2021 (https://n.neurology.org/content/96/15_Supplement/2093).

This study was supported in part by the U.S. National Human Genome Research Institute (NHGRI) and National Heart Lung and Blood Institute (NHBLI) to the Baylor-Hopkins Center for Mendelian Genomics (BHCMG, UM1 HG006542, J.R.L); NHGRI grant to Baylor College of Medicine Human Genome Sequencing Center (U54HG003273 to R.A.G.), U.S. National Institute of Neurological Disorders and Stroke (NINDS)

(R35NS105078 to J.R.L. and R01NS106298 to M.C.K.), Spastic Paraplegia Foundation (SPF) (to J.R.L.), and Muscular Dystrophy Association (MDA) (512848 to J.R.L.). The functional studies performed for Family 20 were supported by the Care4Rare Canada Consortium funded by Genome Canada and the Ontario Genomics Institute (OGI-147), the Canadian Institutes of Health Research, Ontario Research Fund, Genome Alberta, Genome British Columbia, Genome Quebec, and Children's Hospital of Eastern Ontario Foundation. S.B. is supported by a Cerebral Palsy Alliance Research Foundation Career Development Award. SCR is supported by: National Institute of Health (R01 DK108894; R21 CA164970 and R21 CA221702) and USA Department of Defense Award (W81XWH-16-0464). D.M. was supported by a Medical Genetics Research Fellowship Program through the United States National Institute of Health (T32 GM007526-42). T.M. was supported by the Uehara Memorial Foundation. D.P. is supported by a Clinical Research Training Scholarship in Neuromuscular Disease by the American Brain Foundation (ABF) and Muscle Study Group (MSG), and International Rett Syndrome Foundation (IRSF grant #3701-1). J.E.P. was supported by NHGRI K08 HG008986. D.G.C. is supported by NIH – Brain Disorders and Development Training Grant (T32 NS043124-19). A.E.M. is supported by a Canadian Institutes of Health Research (CIHR) fellowship award (MFE-176616). J.A.M.S. is supported by Conselho Nacional de Desenvolvimento Científico e Tecnológico (CNPq). V.M. was supported in part by the Karl Kahane Foundation. A.L. was supported in part by the Israeli MOH grant (#5914) and the Israeli MOH/ERA-Net (#4800). TSB is supported by the Netherlands Organization for Scientific Research (ZonMW Veni, grant 91617021), a NARSAD Young Investigator Grant from the Brain & Behavior Research Foundation, an Erasmus MC Fellowship 2017, and Erasmus MC Human Disease Model Award 2018.

Author Contributions

DGC, IH, and JRL contributed to the conception and design of the study; DGC, IH, AEM, RM, KCD, JMF, TM, HD, CMG, SS, CG, SB, YAI, CR, JVH, VRS, LTE, KMB, AL, YF, EP, YK, VM, MS, CR, KM, NWS, MSZ, AB, TSB, DLS, MO, TOS, HH, DM, EGK, YJ, AGJ, HT, SCJ, MRA, REV, SH, SA, AB, EZ, MMS, NAS, GZ, PB, SR, ZCA, LT, FC, SNJ, RAG, JEP, MCK, KDK, JAMS, AV, SHE, DP, DM, JRL contributed to the acquisition and analysis of the data; DGC, IH contributed to drafting of the text and preparing the figures. All authors approved the final manuscript.

Potential conflicts of interests

Nothing to report.

References

1. Lupski, J.R., Liu, P., Stankiewicz, P., Carvalho, C.M.B., and Posey, J.E. (2020). Clinical genomics and contextualizing genome variation in the diagnostic laboratory. Expert Rev Mol Diagn *20*, 995-1002. 10.1080/14737159.2020.1826312.

2. Karaca, E., Posey, J.E., Coban Akdemir, Z., Pehlivan, D., Harel, T., Jhangiani, S.N., Bayram, Y., Song, X., Bahrambeigi, V., Yuregir, O.O., et al. (2018). Phenotypic expansion illuminates multilocus pathogenic variation. Genet Med *20*, 1528-1537. 10.1038/gim.2018.33.

3. Mitani, T., Isikay, S., Gezdirici, A., Gulec, E.Y., Punetha, J., Fatih, J.M., Herman, I., Akay, G., Du, H., Calame, D.G., et al. (2021). High prevalence of multilocus pathogenic variation in neurodevelopmental disorders in the Turkish population. Am J Hum Genet *108*, 1981-2005. 10.1016/j.ajhg.2021.08.009.

4. Ruano, L., Melo, C., Silva, M.C., and Coutinho, P. (2014). The global epidemiology of hereditary ataxia and spastic paraplegia: a systematic review of prevalence studies. Neuroepidemiology *42*, 174-183. 10.1159/000358801.

5. Blackstone, C. (2018). Hereditary spastic paraplegia. Handb Clin Neurol *148*, 633-652. 10.1016/b978-0-444-64076-5.00041-7.

6. Novarino, G., Fenstermaker, A.G., Zaki, M.S., Hofree, M., Silhavy, J.L., Heiberg, A.D., Abdellateef, M., Rosti, B., Scott, E., Mansour, L., et al. (2014). Exome sequencing links corticospinal motor neuron disease to common neurodegenerative disorders. Science *343*, 506-511. 10.1126/science.1247363.

7. Blackstone, C. (2018). Converging cellular themes for the hereditary spastic paraplegias. Curr Opin Neurobiol *51*, 139-146. 10.1016/j.conb.2018.04.025.

8. Harding, A.E. (1993). Hereditary spastic paraplegias. Semin Neurol *13*, 333-336. 10.1055/s-2008-1041143.

9. Fink, J.K. (2013). Hereditary spastic paraplegia: clinico-pathologic features and emerging molecular mechanisms. Acta Neuropathol *126*, 307-328. 10.1007/s00401-013-1115-8.

10. DiVincenzo, C., Elzinga, C.D., Medeiros, A.C., Karbassi, I., Jones, J.R., Evans, M.C., Braastad, C.D., Bishop, C.M., Jaremko, M., Wang, Z., et al. (2014). The allelic spectrum of Charcot-Marie-Tooth disease in over 17,000 individuals with neuropathy. Mol Genet Genomic Med *2*, 522-529. 10.1002/mgg3.106.

11. Salinas, S., Proukakis, C., Crosby, A., and Warner, T.T. (2008). Hereditary spastic paraplegia: clinical features and pathogenetic mechanisms. Lancet Neurol *7*, 1127-1138. 10.1016/S1474-4422(08)70258-8.

12. Shribman, S., Reid, E., Crosby, A.H., Houlden, H., and Warner, T.T. (2019). Hereditary spastic paraplegia: from diagnosis to emerging therapeutic approaches. Lancet Neurol *18*, 1136-1146. 10.1016/s1474-4422(19)30235-2.

13. Burguez, D., Polese-Bonatto, M., Scudeiro, L.A.J., Björkhem, I., Schöls, L., Jardim, L.B., Matte, U., Saraiva-Pereira, M.L., Siebert, M., and Saute, J.A.M. (2017). Clinical

and molecular characterization of hereditary spastic paraplegias: A next-generation sequencing panel approach. J Neurol Sci *383*, 18-25. 10.1016/j.jns.2017.10.010.

14. Schule, R., Wiethoff, S., Martus, P., Karle, K.N., Otto, S., Klebe, S., Klimpe, S., Gallenmuller, C., Kurzwelly, D., Henkel, D., et al. (2016). Hereditary spastic paraplegia: Clinicogenetic lessons from 608 patients. Ann Neurol *79*, 646-658. 10.1002/ana.24611.

15. Boone, P.M., Liu, P., Zhang, F., Carvalho, C.M., Towne, C.F., Batish, S.D., and Lupski, J.R. (2011). Alu-specific microhomology-mediated deletion of the final exon of SPAST in three unrelated subjects with hereditary spastic paraplegia. Genet Med *13*, 582-592. 10.1097/GIM.0b013e3182106775.

16. Mamelona, J., Crapoulet, N., and Marrero, A. (2019). A new case of spastic paraplegia type 64 due to a missense mutation in the ENTPD1 gene. Hum Genome Var *6*, 5. 10.1038/s41439-018-0036-4.

17. Travaglini, L., Aiello, C., Stregapede, F., D'Amico, A., Alesi, V., Ciolfi, A., Bruselles, A., Catteruccia, M., Pizzi, S., Zanni, G., et al. (2018). The impact of next-generation sequencing on the diagnosis of pediatric-onset hereditary spastic paraplegias: new genotype-phenotype correlations for rare HSP-related genes. Neurogenetics *19*, 111-121. 10.1007/s10048-018-0545-9.

18. Pashaei, M., Davarzani, A., Hajati, R., Zamani, B., Nafissi, S., Larti, F., Nilipour, Y., Rohani, M., and Alavi, A. (2021). Description of clinical features and genetic analysis of one ultra-rare (SPG64) and two common forms (SPG5A and SPG15) of hereditary spastic paraplegia families. J Neurogenet, 1-11. 10.1080/01677063.2021.1895146.

19. Wohler, E., Martin, R., Griffith, S., da S. Rodrigues, E., Antonescu, C., Posey, J.E., Coban-Akdemir, Z., Jhangiani, S.N., Doheny, K.F., Lupski, J.R., Valle, D., Hamosh, A., Sobreira, N. (2021). PhenoDB, GeneMatcher and VariantMatcher, tools for analysis

and sharing of sequence data. Orphanet J Rare Dis. https://doi.org/10.1186/s13023-021-01916-z.

20. Köhler, S., Vasilevsky, N.A., Engelstad, M., Foster, E., McMurry, J., Aymé, S., Baynam, G., Bello, S.M., Boerkoel, C.F., Boycott, K.M., et al. (2017). The Human Phenotype Ontology in 2017. Nucleic Acids Res *45*, D865-d876. 10.1093/nar/gkw1039.

21. Karaca, E., Harel, T., Pehlivan, D., Jhangiani, S.N., Gambin, T., Coban Akdemir, Z., Gonzaga-Jauregui, C., Erdin, S., Bayram, Y., Campbell, I.M., et al. (2015). Genes that Affect Brain Structure and Function Identified by Rare Variant Analyses of Mendelian Neurologic Disease. Neuron *88*, 499-513. 10.1016/j.neuron.2015.09.048.

22. Perenthaler, E., Nikoncuk, A., Yousefi, S., Berdowski, W.M., Alsagob, M., Capo, I., van der Linde, H.C., van den Berg, P., Jacobs, E.H., Putar, D., et al. (2020). Loss of UGP2 in brain leads to a severe epileptic encephalopathy, emphasizing that bi-allelic isoform-specific start-loss mutations of essential genes can cause genetic diseases. Acta Neuropathol *139*, 415-442. 10.1007/s00401-019-02109-6.

23. Kennedy, A.D., Pappan, K.L., Donti, T.R., Evans, A.M., Wulff, J.E., Miller, L.A.D., Reid Sutton, V., Sun, Q., Miller, M.J., and Elsea, S.H. (2017). Elucidation of the complex metabolic profile of cerebrospinal fluid using an untargeted biochemical profiling assay. Mol Genet Metab *121*, 83-90. 10.1016/j.ymgme.2017.04.005.

24. Miller, M.J., Kennedy, A.D., Eckhart, A.D., Burrage, L.C., Wulff, J.E., Miller, L.A., Milburn, M.V., Ryals, J.A., Beaudet, A.L., Sun, Q., et al. (2015). Untargeted metabolomic analysis for the clinical screening of inborn errors of metabolism. J Inherit Metab Dis *38*, 1029-1039. 10.1007/s10545-015-9843-7.

25. Ford, L., Kennedy, A.D., Goodman, K.D., Pappan, K.L., Evans, A.M., Miller, L.A.D., Wulff, J.E., Wiggs, B.R., Lennon, J.J., Elsea, S., and Toal, D.R. (2020). Precision of a

Clinical Metabolomics Profiling Platform for Use in the Identification of Inborn Errors of Metabolism. J Appl Lab Med *5*, 342-356. 10.1093/jalm/jfz026.

26. Alaimo, J.T., Glinton, K.E., Liu, N., Xiao, J., Yang, Y., Reid Sutton, V., and Elsea, S.H. (2020). Integrated analysis of metabolomic profiling and exome data supplements sequence variant interpretation, classification, and diagnosis. Genet Med *22*, 1560-1566. 10.1038/s41436-020-0827-0.

27. Liu, N., Xiao, J., Gijavanekar, C., Pappan, K.L., Glinton, K.E., Shayota, B.J., Kennedy, A.D., Sun, Q., Sutton, V.R., and Elsea, S.H. (2021). Comparison of Untargeted Metabolomic Profiling vs Traditional Metabolic Screening to Identify Inborn Errors of Metabolism. JAMA Netw Open *4*, e2114155. 10.1001/jamanetworkopen.2021.14155.

28. Wang, T.F., Ou, Y., and Guidotti, G. (1998). The transmembrane domains of ectoapyrase (CD39) affect its enzymatic activity and quaternary structure. J Biol Chem *273*, 24814-24821. 10.1074/jbc.273.38.24814.

29. Hansen, A.W., Murugan, M., Li, H., Khayat, M.M., Wang, L., Rosenfeld, J., Andrews, B.K., Jhangiani, S.N., Coban Akdemir, Z.H., Sedlazeck, F.J., et al. (2019). A Genocentric Approach to Discovery of Mendelian Disorders. Am J Hum Genet *105*, 974-986. 10.1016/j.ajhg.2019.09.027.

30. Inoue, K., Khajavi, M., Ohyama, T., Hirabayashi, S., Wilson, J., Reggin, J.D., Mancias, P., Butler, I.J., Wilkinson, M.F., Wegner, M., and Lupski, J.R. (2004). Molecular mechanism for distinct neurological phenotypes conveyed by allelic truncating mutations. Nat Genet *36*, 361-369. 10.1038/ng1322.

31. Vuerich, M., Robson, S.C., and Longhi, M.S. (2019). Ectonucleotidases in Intestinal and Hepatic Inflammation. Front Immunol *10*, 507. 10.3389/fimmu.2019.00507.

32. Hillard, C.J. (2018). Circulating Endocannabinoids: From Whence Do They Come and Where are They Going? Neuropsychopharmacology *43*, 155-172. 10.1038/npp.2017.130.

33. Najmabadi, H., Hu, H., Garshasbi, M., Zemojtel, T., Abedini, S.S., Chen, W., Hosseini, M., Behjati, F., Haas, S., Jamali, P., et al. (2011). Deep sequencing reveals 50 novel genes for recessive cognitive disorders. Nature *478*, 57-63. 10.1038/nature10423.

34. Kevelam, S.H., Bierau, J., Salvarinova, R., Agrawal, S., Honzik, T., Visser, D., Weiss, M.M., Salomons, G.S., Abbink, T.E., Waisfisz, Q., and van der Knaap, M.S. (2015). Recessive ITPA mutations cause an early infantile encephalopathy. Ann Neurol *78*, 649-658. 10.1002/ana.24496.

35. Wang, Q., Pierce-Hoffman, E., Cummings, B.B., Alföldi, J., Francioli, L.C., Gauthier, L.D., Hill, A.J., O'Donnell-Luria, A.H., Karczewski, K.J., and MacArthur, D.G. (2020). Landscape of multi-nucleotide variants in 125,748 human exomes and 15,708 genomes. Nat Commun *11*, 2539. 10.1038/s41467-019-12438-5.

36. Gonzaga-Jauregui, C., Yesil, G., Nistala, H., Gezdirici, A., Bayram, Y., Nannuru, K.C., Pehlivan, D., Yuan, B., Jimenez, J., Sahin, Y., et al. (2020). Functional biology of the Steel syndrome founder allele and evidence for clan genomics derivation of COL27A1 pathogenic alleles worldwide. Eur J Hum Genet *28*, 1243-1264. 10.1038/s41431-020-0632-x.

37. Lupski, J.R., Belmont, J.W., Boerwinkle, E., and Gibbs, R.A. (2011). Clan genomics and the complex architecture of human disease. Cell *147*, 32-43. 10.1016/j.cell.2011.09.008.

38. Howe, K.L., Achuthan, P., Allen, J., Allen, J., Alvarez-Jarreta, J., Amode, M.R., Armean, I.M., Azov, A.G., Bennett, R., Bhai, J., et al. (2021). Ensembl 2021. Nucleic Acids Res *49*, D884-d891. 10.1093/nar/gkaa942.

39. Rinaldi, C., and Wood, M.J.A. (2018). Antisense oligonucleotides: the next frontier for treatment of neurological disorders. Nat Rev Neurol *14*, 9-21. 10.1038/nrneurol.2017.148.

40. Badimon, A., Strasburger, H.J., Ayata, P., Chen, X., Nair, A., Ikegami, A., Hwang, P., Chan, A.T., Graves, S.M., Uweru, J.O., et al. (2020). Negative feedback control of neuronal activity by microglia. Nature *586*, 417-423. 10.1038/s41586-020-2777-8.

41. Pankratov, Y., Lalo, U., Verkhratsky, A., and North, R.A. (2006). Vesicular release of ATP at central synapses. Pflugers Arch *452*, 589-597. 10.1007/s00424-006-0061-x.

42. Cieślak, M., Roszek, K., and Wujak, M. (2019). Purinergic implication in amyotrophic lateral sclerosis-from pathological mechanisms to therapeutic perspectives. Purinergic Signal *15*, 1-15. 10.1007/s11302-018-9633-4.

43. Nobbio, L., Sturla, L., Fiorese, F., Usai, C., Basile, G., Moreschi, I., Benvenuto, F., Zocchi, E., De Flora, A., Schenone, A., and Bruzzone, S. (2009). P2X7-mediated increased intracellular calcium causes functional derangement in Schwann cells from rats with CMT1A neuropathy. J Biol Chem *284*, 23146-23158. 10.1074/jbc.M109.027128.

44. Nardi-Schreiber, A., Sapir, G., Gamliel, A., Kakhlon, O., Sosna, J., Gomori, J.M., Meiner, V., Lossos, A., and Katz-Brull, R. (2017). Defective ATP breakdown activity related to an ENTPD1 gene mutation demonstrated using (31)P NMR spectroscopy. Chem Commun (Camb) *53*, 9121-9124. 10.1039/c7cc00426e.

45. Wu, J.J., Choi, L.E., and Guidotti, G. (2005). N-linked oligosaccharides affect the enzymatic activity of CD39: diverse interactions between seven N-linked glycosylation sites. Mol Biol Cell *16*, 1661-1672. 10.1091/mbc.e04-10-0886.

46. Corti, F., Olson, K.E., Marcus, A.J., and Levi, R. (2011). The expression level of ecto-NTP diphosphohydrolase1/CD39 modulates exocytotic and ischemic release of

neurotransmitters in a cellular model of sympathetic neurons. J Pharmacol Exp Ther *337*, 524-532. 10.1124/jpet.111.179994.

47. Lanser, A.J., Rezende, R.M., Rubino, S., Lorello, P.J., Donnelly, D.J., Xu, H., Lau, L.A., Dulla, C.G., Caldarone, B.J., Robson, S.C., and Weiner, H.L. (2017). Disruption of the ATP/adenosine balance in CD39(-/-) mice is associated with handling-induced seizures. Immunology *152*, 589-601. 10.1111/imm.12798.

48. Enjyoji, K., Sévigny, J., Lin, Y., Frenette, P.S., Christie, P.D., Esch, J.S., 2nd, Imai, M., Edelberg, J.M., Rayburn, H., Lech, M., et al. (1999). Targeted disruption of cd39/ATP diphosphohydrolase results in disordered hemostasis and thromboregulation. Nat Med *5*, 1010-1017. 10.1038/12447.

49. Deaglio, S., Dwyer, K.M., Gao, W., Friedman, D., Usheva, A., Erat, A., Chen, J.F., Enjyoji, K., Linden, J., Oukka, M., et al. (2007). Adenosine generation catalyzed by CD39 and CD73 expressed on regulatory T cells mediates immune suppression. J Exp Med *204*, 1257-1265. 10.1084/jem.20062512.

50. Friedman, D.J., Künzli, B.M., YI, A.R., Sevigny, J., Berberat, P.O., Enjyoji, K., Csizmadia, E., Friess, H., and Robson, S.C. (2009). From the Cover: CD39 deletion exacerbates experimental murine colitis and human polymorphisms increase susceptibility to inflammatory bowel disease. Proc Natl Acad Sci U S A *106*, 16788-16793. 10.1073/pnas.0902869106.

51. Schüle, R., Holland-Letz, T., Klimpe, S., Kassubek, J., Klopstock, T., Mall, V., Otto, S., Winner, B., and Schöls, L. (2006). The Spastic Paraplegia Rating Scale (SPRS): a reliable and valid measure of disease severity. Neurology *67*, 430-434. 10.1212/01.wnl.0000228242.53336.90.

Figure legends

Figure 1 Pedigrees and variant information for families with *ENTPD1*-related neurological disease. (**A**) Pedigree and Sanger sequencing results of index family 1 with the homozygous variant NM_001766.6: c.398_399delinsAA; p.(Gly133Glu). (**B**) Absence of heterozygosity (AOH) plot of P1 showing a total AOH size of 310 Mb and 11.1 Mb of AOH around *ENTPD1*: c.398_399delinsAA (red line). (**C**) Pedigrees and variant information of newly identified families with biallelic *ENTPD1* variants and countries of origin.

Figure 2 Representative photographs and radiographs of individuals with *ENTPD1*-related neurological disease. (**A**) Facial pictures of affected individuals showing low anterior hairline, synophrys, low-set ears with fleshy lobes, prominent philtrum, and micrognathia. (**B**) Pictures of P1 at 8 years of age and P21 at 8 years showing centripetal obesity, thoracic kyphosis, decreased lumbar lordosis, genu valgus, and cubitus valgus. (**C**) Representative hand images of P1, P4, P8, and P24 showing broad fingers with camptodactyly and spatulated finger tips (**D**) Representative foot images of P1, P4, and P8 at 8, 15, and 3 years, respectively, showing broad toes with camptodactyly (P1), *pes cavus* with camptodactyly (P4), and broad great toes bilaterally and broad right 4th toe with camptodactyly (P8). (**E**) Hand radiographs of P1 at 8 years of age showing severe camptodactyly. (**F**) Foot radiographs of P1 at 8 years showing camptodactyly. (**G**) Foot radiographs of P5 at 15 years showing *pes cavus* and camptodactyly. (**H**) Foot radiographs of P34 at 19 years of age showing severe camptodactyly. (**I**) Sagittal spine radiograph of P1 at 8 years showing lumbar lordosis. (**J**) Hip radiograph of P8 at 3 years showing no gross abnormalities.

Figure 3 Individuals with biallelic pathogenic *ENTPD1* variants show white matter abnormalities, thinning of the corpus callosum, cerebellar atrophy, and signal abnormalities in posterior limb of the internal capsule. Representative magnetic resonance imaging (MRI) of the brain of affected individuals from different families at different ages. Arrows in the axial images are highlighting abnormal signal hyperintensity of the posterior limb of the internal capsule. (**A**) Sagittal T1-weighted imaging (1) and axial T2-FLAIR of P7 at 17 years of age. (**B**) and (**C**) Sagittal T1-weighted imaging (1) and axial T2-FLAIR of P8 at 3 and 4 years, respectively. (**D**) Sagittal T1-weighted imaging (1) and axial T2-FLAIR of P9 at 3 years. (**E**) Sagittal T2-weighted imaging (1) and axial T2-FLAIR of P16 at 7 years. (F) Sagittal (1) and axial (2) T2-weighted imaging of P23 at 8 years, G) Sagittal T1-weighted imaging (1) and axial T2 of P34 at 15 years.

Figure 4 Biallelic pathogenic *ENTPD1* variants identified in this cohort. (**A**) Schematic showing chromosomal location and gene structure of *ENTPD1*. Previously unreported variants are labeled in red and previously published variants in black. (B) Linear amino acid structure of ENTPD1 and location of previously unreported (red) and published variant alleles (black).

Figure 5 Alternative splicing due to *ENTPD1*:c.574-6_574-3del results in skipping of exon 6. (**A**) Schematic of *ENTPD1* NM_001776.6, the most widely expressed trancript, showing 10 different exons. *ENTPD1*: c.574-6_574-3del is located in intron 5 (red asterisk). Arrows show location of primers for cDNA amplification. (**B**) Agarose gel electrophoresis image of *ENTPD1* cDNA exon 4F and 7R amplification and schematic of resultant splicing products. Unaffected wildtype control cDNA and heterozygous parental cDNA show amplification of a bands at 818 bp not found in the affected proband sample (P15). Sanger

sequencing confirmed that the 818 bp band contains exons 4, 5, 6, and 7 in control and unaffected parent. By contrast, the proband P15 who carries the homozygous *ENTPD1*: c.574-6_574-3del variant contains an alternative 572 bp product including exons 4, 5, and 7 only and thus skipping exon 6 completely. All three samples additionally contain a smaller product at 412 bp only containing exons 4 and 7. (**C**) Agarose gel electrophoresis image of *ENTPD1* cDNA exon 6F and 10R amplification. Unaffected wildtype control cDNA and heterozygous parental cDNA show amplification of an 861 bp band containing exons 6, 7, 8, 9, and 10. No amplification is present in the homozygous proband sample.

Figure 6 Biallelic *ENTPD1* variants impair ATP hydrolysis and ENTPD1 expression. (**A**) ATP metabolic pathway showing the role of ENTPD1 in hydrolysis of ATP to ADP and ADP to AMP. (**B**) Lymphoblasts were derived from family 20 with two affected siblings (P32 and P33 with homozygous *ENTPD1*:c.401T>G; p.(Met134Arg) variant. (**C**) Reverse transcription-quantitative PCR of ENTPD1 mRNA levels, using primers spanning both exons 1-2 and exons 9-10 showing significantly decreased ENTPD1 mRNA levels in lymphoblasts from individuals with homozygous *ENTPD1*:c.401T>G variant. (**D**) Western blot of ENTPD1 p.(Met134Arg) showing deceased protein levels in patient lymphoblasts. The stain-free gel serves as the loading control. (**E**) Measured ATPase and ADPase activity using normalized phosphate production after incubation with either ATP or ADP at a final concentration of 10 mM for 30 min. * $p<0.05$. (**F**) Flow cytometry of ENTPD1+ lymphocytes and polymorphonuclear leukocytes (PMNs) in blood samples from P12 and P13 with homozygous *ENTPD1*:c.185T>G; p.(Leu62*) variant compared to control and heterozygous parental samples. (**G**) Immunohistochemical staining for ENTPD1 performed on paraffin sections of sural nerve biopsy from P12 with variant *ENTPD1*:c.185T>G shows complete absence of endo- and epineural vascular staining compared to control sample.

Figure 7 ENTPD1 deficiency alters multiple metabolic pathways important for lipid and energy metabolism. (**A**) Metabolite Enrichment (left) illustrates molecule distribution of specific perturbed metabolites altered in at least 2/3 of tested individuals (n = 37). Pathway Enrichment (right) illustrates altered molecules from the same metabolic pathways (n = 148). In Pathway Enrichment, molecules may or may not be identical between patient samples; however, molecules fall within the same metabolic pathway. The distribution of these molecules across all patient samples illustrates the broader impact of lipid and energy metabolism due to ENTPD1 deficiency. (**B**) Gene-Metabolite Disease Pathway Interaction is shown for significantly perturbed metabolites in plasma was patient with ENTPD1 deficiency. Metabolites assessed (n = 98) are limited to molecules mapped to KEGG pathways. The most significantly altered pathways ($p = <0.05$) are labeled.

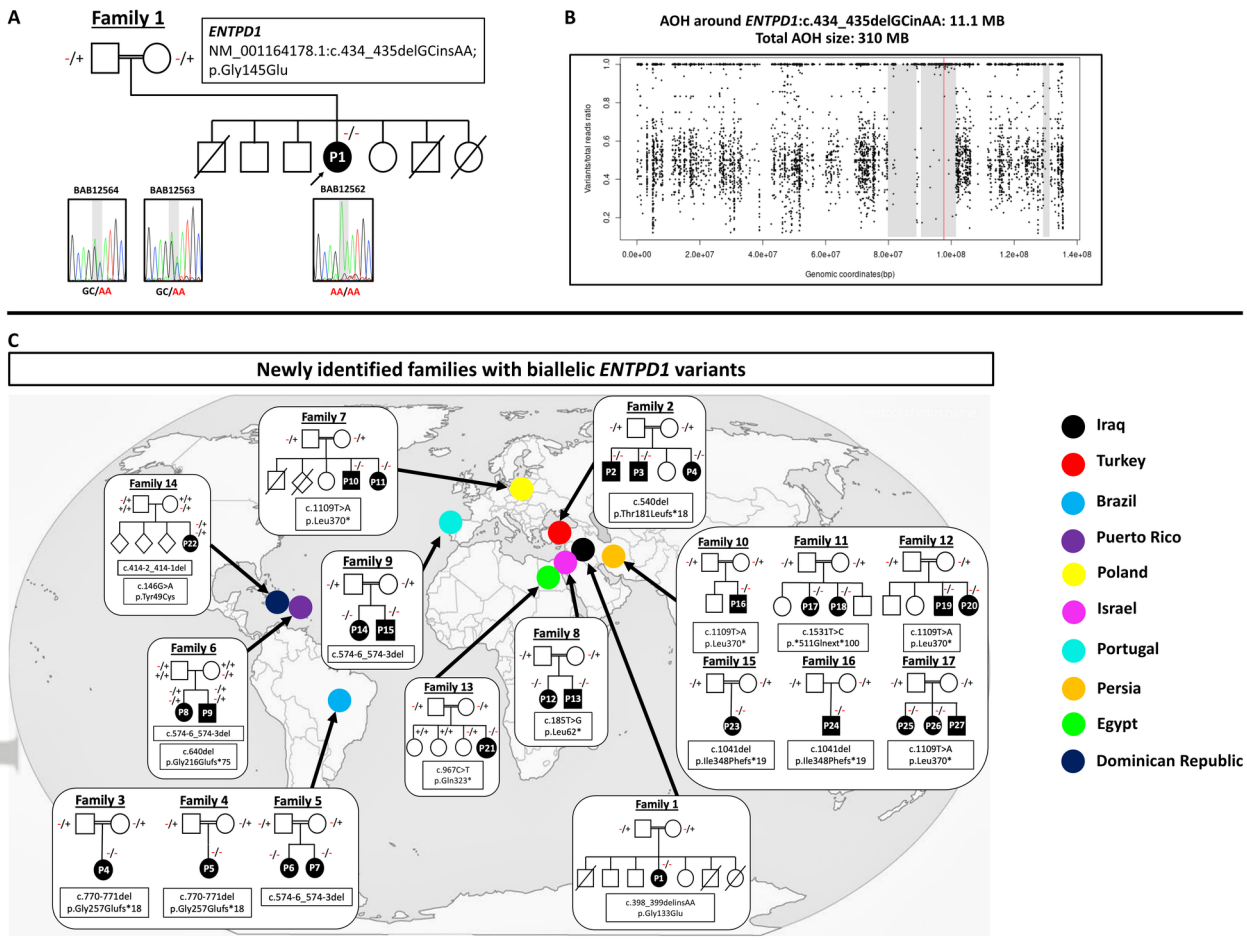

Figure 1 with World Map.TIF

Figure 2 Pics and Xrays.275.tif

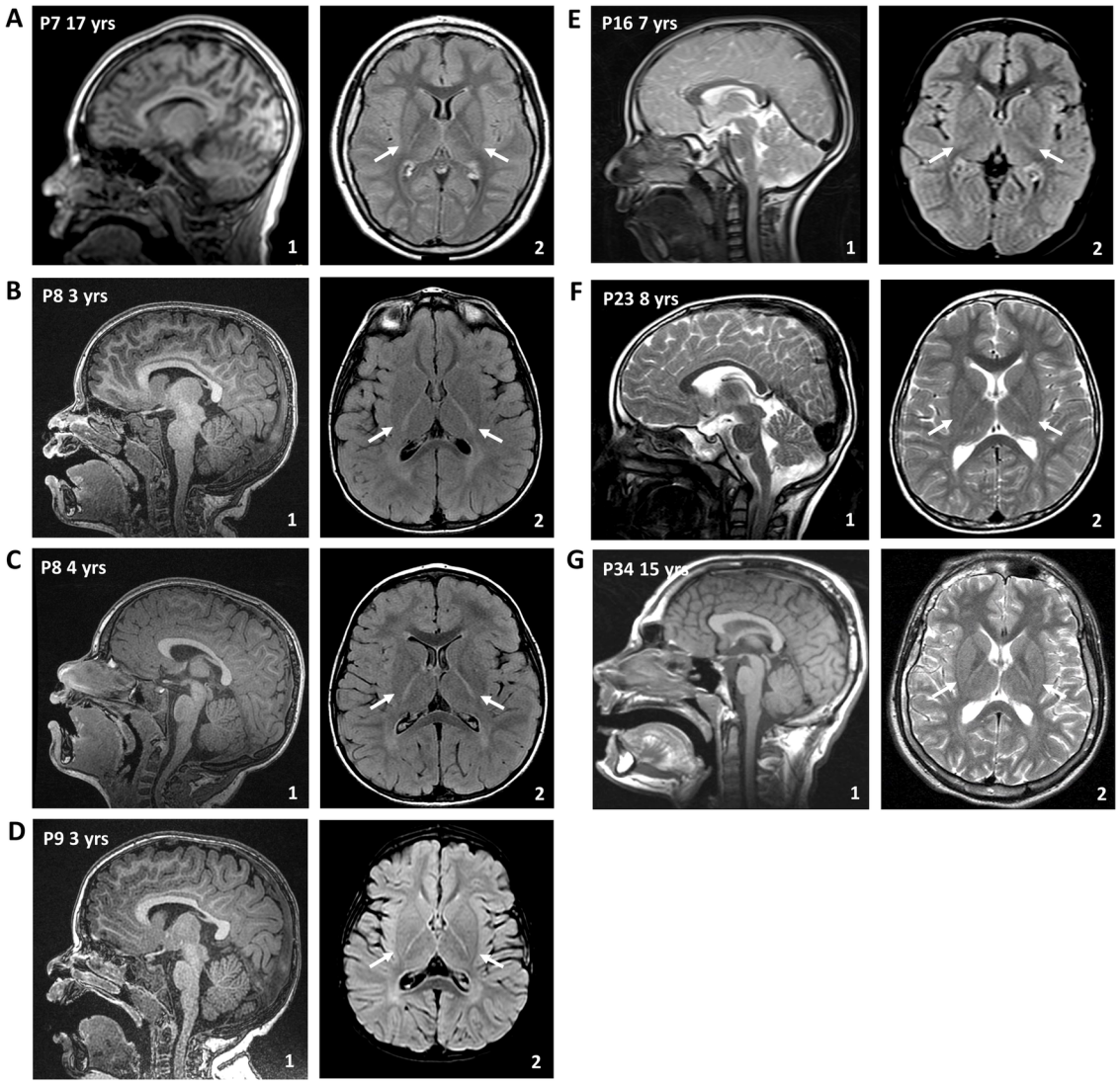

Figure 3 MRI images.TIF

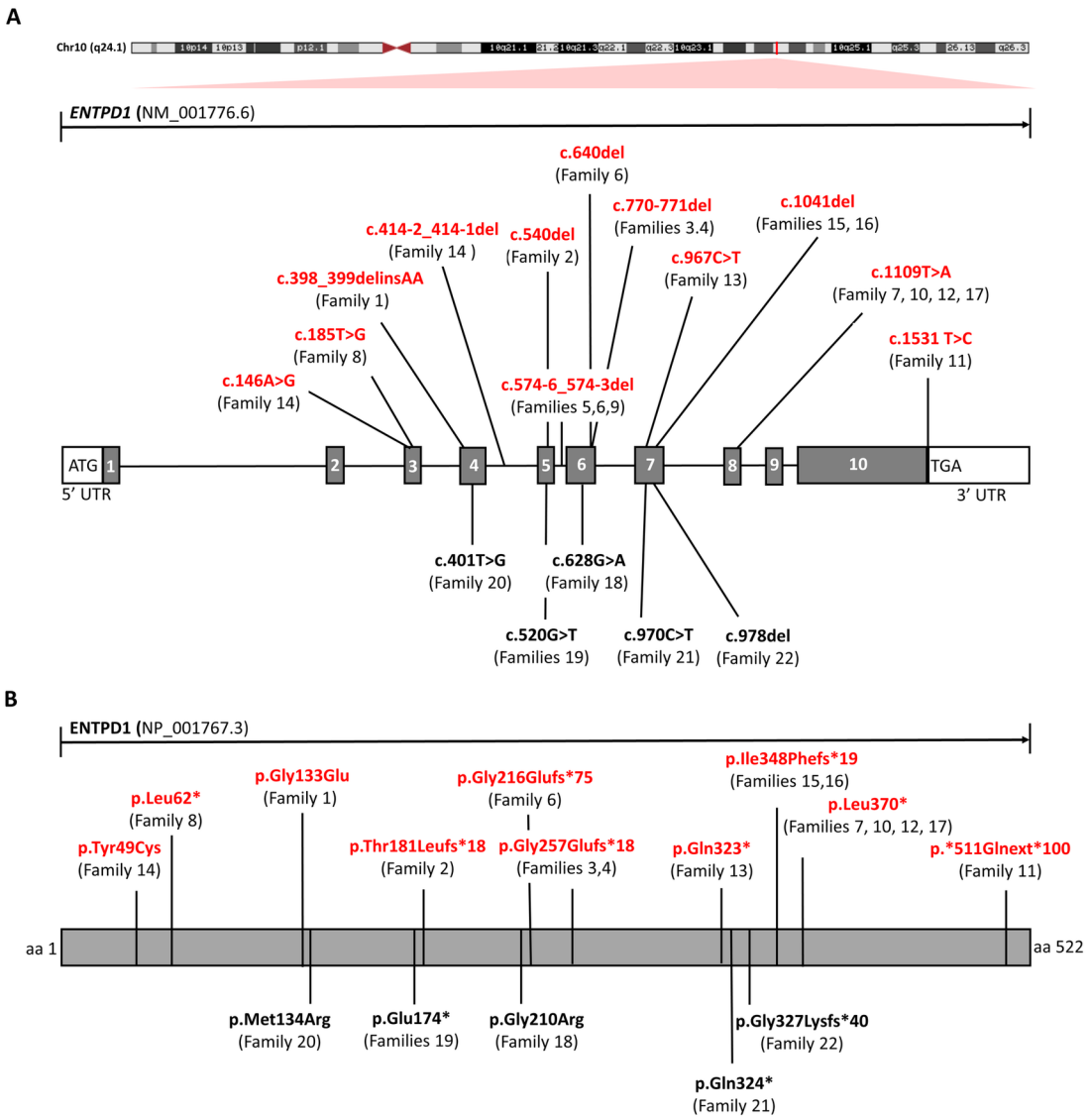

Figure 4.TIF

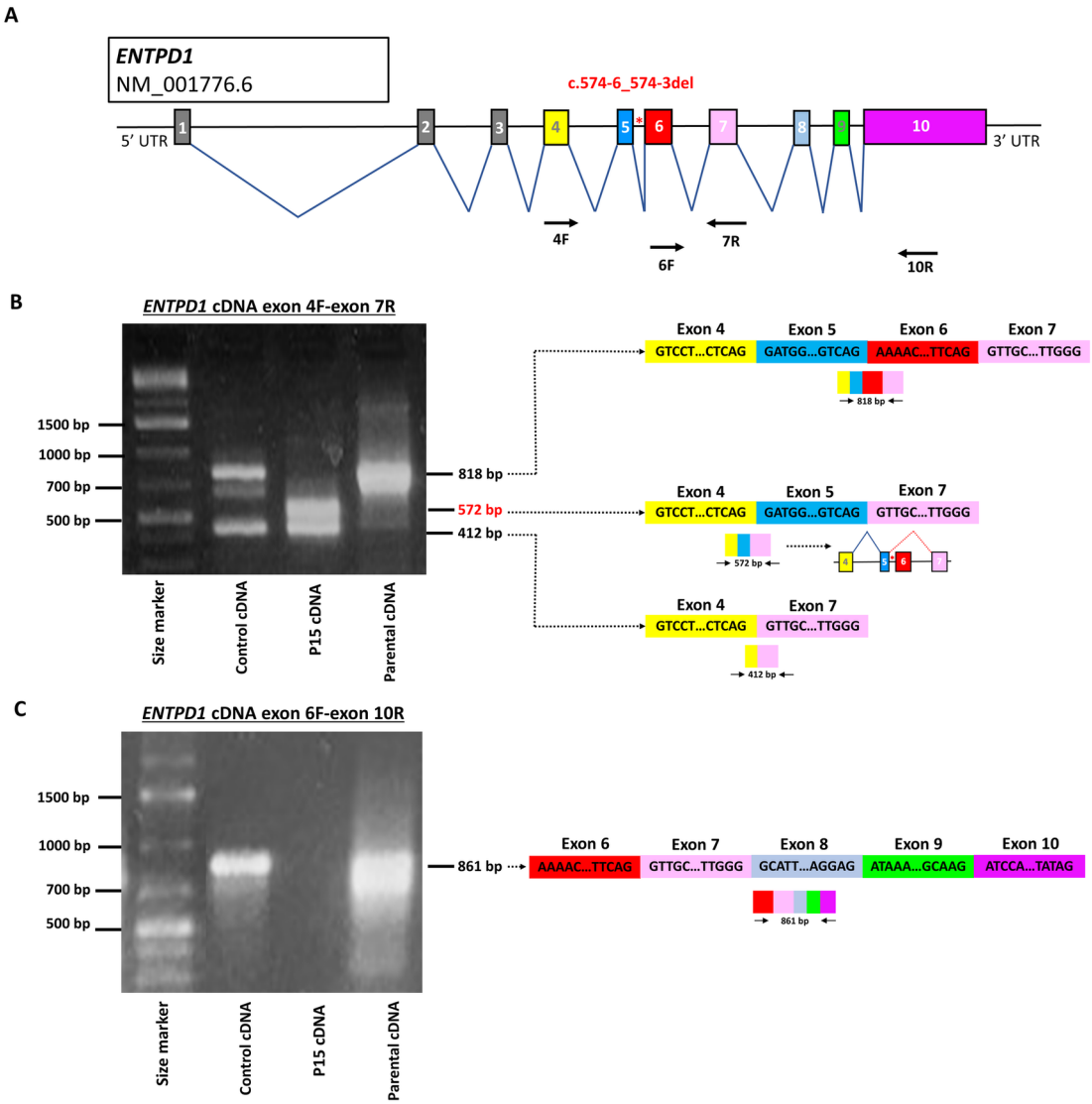

Figure 5.TIF

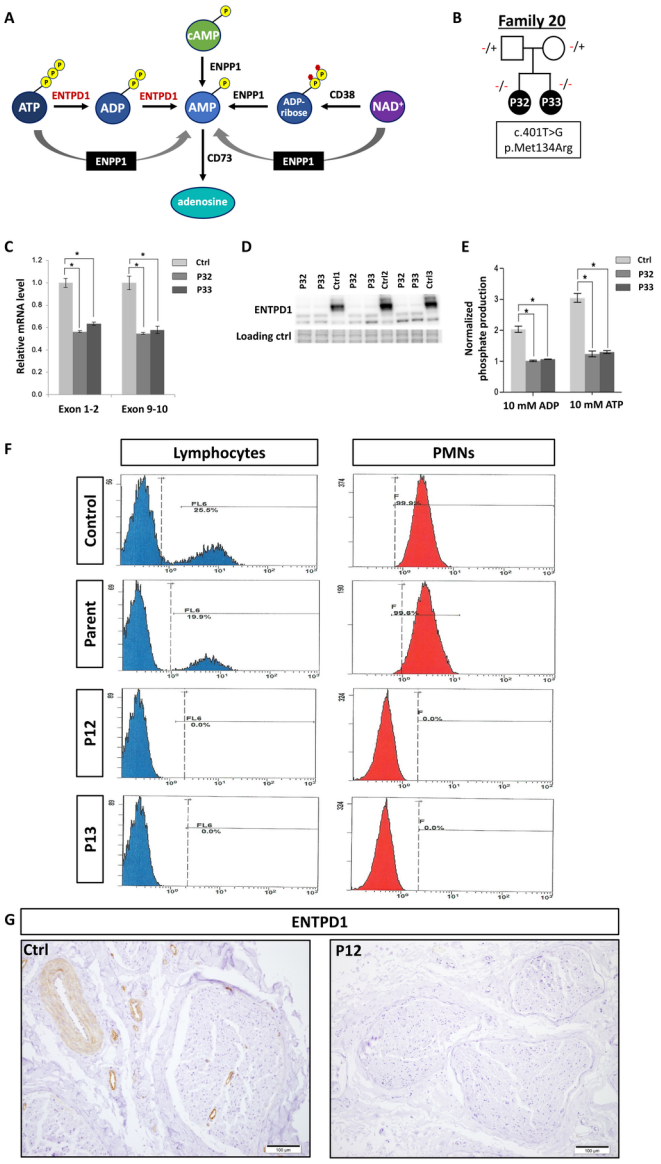

Figure 6 Functional studies.tif

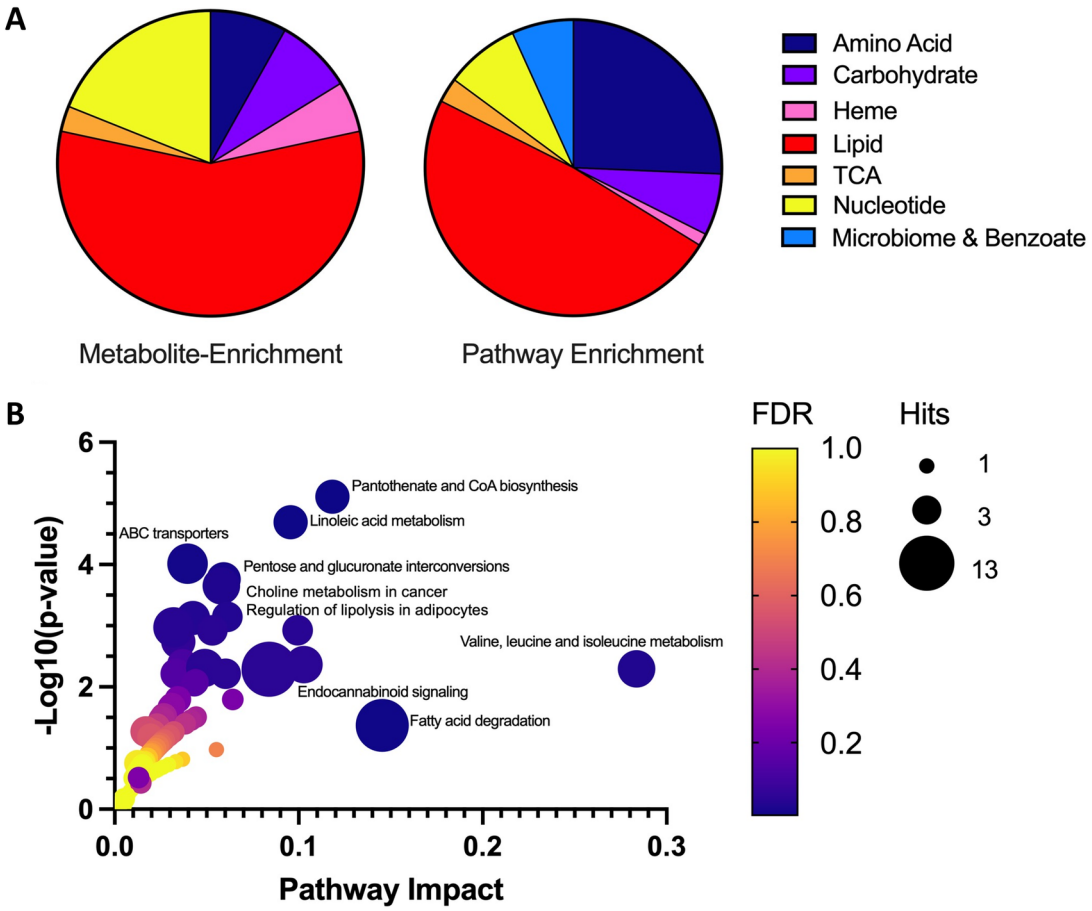

Figure 7.TIF

Table 1 Phenotypic features of *ENTPD1*-related neurological disease

Clinical features	This cohort	Prior publications	All affected individuals
Early childhood age of onset (HP:0011463)	27/27	9/9	36/36
Developmental delay/intellectual disability (HP:0012758)	27/27	9/9	36/36
Progressive spastic paraplegia (HP:0007020)	27/27	9/9	36/36
Gait impairment (HP:0002355)	27/27	9/9	36/36
Weakness (HP:0001324)	23/27	5/9	28/36
Dysarthria (HP:0001260)	20/27	7/9	27/36
Abnormal reflexes (HP:0031826)	18/27	9/9	27/36
Neurocognitive regression (HP:0002376)	18/27	3/9	21/36
Behavioural abnormalities (HP:0000708)	17/27	7/9	22/36
Hand and foot deformities (HP:0001155 and 0001760)	15/27	4/9	19/36
Neuropathy (HP:0009830)	14/27	4/9	18/36
Spasticity (HP:0001257)	14/27	7/9	21/36
Dysmorphic facies (HP:0001999)	13/27	0/9	13/36
Cerebral white matter abnormalities (HP:0002500)	12/22	3/6	15/28*
Hypotonia (HP:0001252)	7/27	0/9	7/36
Epilepsy (HP:0001250)	7/27	0/9	7/36
Scoliosis (HP:0002650)	5/27	0/9	5/36
Cataracts (HP:0000518)	3/27	1/9	4/36
Cerebellar atrophy (HP:0001272)	2/22	0/6	2/28*

*MRI brain images and/or reports only available for 28/36 individuals